

# Synthesis of Fe-substituted Al-mordenites by hydrothermal method

A. NAKAHIRA, S. NISHIMURA, H. ARITANI

*Kyoto Institute of Technology, Matsugasaki, Sakyo-ku, Kyoto 606-8585, Japan*

*E-mail: nakahira@ipc.kit.ac.jp*

T. YAMAMOTO

*Faculty of Engineering, Kyoto University, Yoshidahoncho, Sakyo-ku, Kyoto 606-8301, Japan*

S. UEDA

*ISIR, Osaka University, Mihogaoka, Ibaraki 567-0047, Japan*

Al-mordenite and Fe-mordenite were synthesized with the tetraethylammonium as a template by hydrothermal method at 150°C in the Na<sub>2</sub>O–Al<sub>2</sub>O<sub>3</sub>–SiO<sub>2</sub>–H<sub>2</sub>O and Na<sub>2</sub>O–Fe<sub>2</sub>O<sub>3</sub>–SiO<sub>2</sub>–H<sub>2</sub>O system, respectively. Synthesis of several Al-mordenites substituted with Fe, Al/Fe ratio = 75/25, 50/50, 25/75, were also attempted in the Na<sub>2</sub>O–Al<sub>2</sub>O<sub>3</sub>–Fe<sub>2</sub>O<sub>3</sub>–SiO<sub>2</sub>–H<sub>2</sub>O system under the same conditions by the hydrothermal method. The continuous solid solution of Fe in Al-mordenite was successfully obtained in mordenites with various Al-Fe molar ratios. Al-mordenite crystal was tablet-like with approximately 20–30 μm in diameter and 5–10 μm in thickness. Fiber-like Fe-mordenite grew up to 20–30 μm in length and 5 μm in diameter. The morphology of Fe-substituted Al-mordenite was cubic-like with 5–10 μm in size. The size of Fe-substituted Al-mordenite decreased with the increase of Fe-content. © 2001 Kluwer Academic Publishers

## 1. Introduction

Natural zeolites often contain some impurities such as cations in the structural framework. Though typical zeolites were composed of both Si-O and Al-O tetrahedron structures, (Al, Si) sites of natural zeolites were often observed to be in part substituted by other elements such as Be, B, Ga, Cr, Fe, Ge etc [1, 2]. Recently much attention was paid to the investigation on the hydrothermal synthesis of a new zeolite, replacing Si and/or Al in the zeolite framework with other atoms, because the substitution of other elements in zeolite structure for Si- and Al-site is expected to develop the novel catalytic properties and expand the application of synthesized zeolite [3, 4]. For example, various types of zeolites substituted by trivalent metal ions were synthesized in order to modify the chemical and catalytic properties [5]. The incorporation of Ga and Be into Al-mordenite and Ge into analcime were successfully synthesized by Ueda *et al.* [6]. Szostak *et al.* reported on the incorporation and stability of iron in molecular sieve silicalite [7].

Chu *et al.* reported that MFI-type ferrisilicate resulted in the control of acidity strength for the oxidation catalyst by the replacement of Fe in the structure [8]. Fe-containing ZSM-5 was showed to be more active in benzene hydroxylation with N<sub>2</sub>O by Kharitonov *et al.* [9]. Recent researchs by Wu *et al.* reported the successful synthesis on the isomorphous substitution of Fe<sup>3+</sup> in the framework of aluminosilicate mor-

denite by hydrothermal method under template-free conditions [10].

In the present paper, the purpose is to synthesize Al-mordenite, Fe-mordenite and Fe-substituted Al-mordenites in the Na<sub>2</sub>O–Al<sub>2</sub>O<sub>3</sub>–Fe<sub>2</sub>O<sub>3</sub>–SiO<sub>2</sub>–H<sub>2</sub>O system with tetraethylammonium as a template. The synthesis of Fe, Al-mordenite with various Al/Fe molar ratios, 75/25, 50/50, 25/75, was tried. Al-mordenite, Fe-mordenite and Fe-substituted Al-mordenites were evaluated by X-ray diffractometer, chemical analysis, and Raman spectrometer. The morphology and shape of various mordenites obtained in this system were observed by SEM.

## 2. Experimental procedure

As a starting material, commercially available silicon powder with purity of 99.999% (Kojundo Chemical Co., Japan) was used for a silicon source. Silicon powder was dissolved with 5 M-NaOH solution at 70°C in a water bath for 24 h. Sodium silicate solution was filtered by a Buchner filter and the residue of the impurities in silicon powder was removed. Aluminium chloride and iron chloride (Wako Junyaku Co., Japan) were used as Al and Fe source, respectively. Aluminium chloride was dissolved with deionized water. Iron chloride was also dissolved with deionized water. Sodium silicate solution and Al and/or Fe solution were thoroughly mixed with 10.5% solution of tetraethylammonium (TEA) as a template and resulted in the homogeneous gel of

mordenite starting material. The contents were transferred to a teflon container in a stainless Morey bomb. The hydrothermal synthesis was performed at 150°C for 4 to 7 days for various gels with Al/Fe molar ratios, 100/0, 75/25, 50/50, 25/75, 0/100. The as-synthesized products were separated by a Buchner filter and thoroughly washed with deionized water and ethanol more than 5 times. Then all solid products were dried in the oven at 50°C for 24 h.

X-ray measurements (XRD) were performed on powder diffractometer with Cu-K $\alpha$  radiation. Thermogravimetric analysis (TG) and differential thermal analysis (DTA) were done on Shimadzu DTG-50 instrument in air atmosphere until 900°C. The temperature increased at the rate of 10°C/min. SEM observation was recorded using a FE-type SEM equipment (Hitachi : S-800). Raman spectra were obtained with a JASCO equipment(NRS-200). Compositions of the products synthesized in this experiment were determined by X-ray fluorescence analysis.

### 3. Results and discussion

Compositions of prepared original gels for Al-mordenite, Fe-mordenite and Fe-substituted Al-mordenites are shown in Table I. The optimum gel composition for single mordenite phase was as follows:

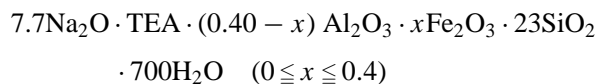


Fig. 1 shows the relation between Fe<sub>2</sub>O<sub>3</sub>/(Al<sub>2</sub>O<sub>3</sub> + Fe<sub>2</sub>O<sub>3</sub>) mole fraction in the starting initial gel materials and in the products. The broken line in Fig. 1 illustrates the variation of mole fraction for ideal Fe-substituted

TABLE I Compositions of prepared original gels for Al-mordenite, Fe-mordenite and Fe-substituted Al-mordenites

Symbol	Al <sub>2</sub> O <sub>3</sub>	Fe <sub>2</sub> O <sub>3</sub>	SiO <sub>2</sub>	Na <sub>2</sub> O	H <sub>2</sub> O	TEA
MOR	0.400	0.000	23	7.7	700	1.0
Fe25	0.300	0.100	23	7.7	700	1.0
Fe50	0.200	0.200	23	7.7	700	1.0
Fe75	0.100	0.300	23	7.7	700	1.0
Fe100	0.000	0.400	23	7.7	700	1.0

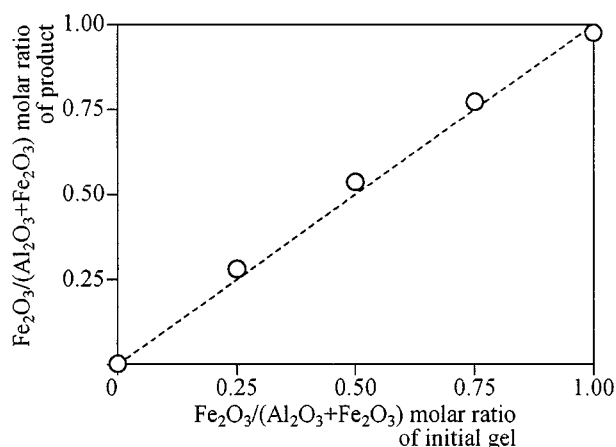


Figure 1 The relation between Fe<sub>2</sub>O<sub>3</sub>/(Al<sub>2</sub>O<sub>3</sub> + Fe<sub>2</sub>O<sub>3</sub>) mole fraction of starting initial materials and the products by hydrothermal process.

Al-mordenites. As shown in Fig. 1, the results indicate the possibility of stoichiometric substitution of Fe for Al in Al-mordenite.

Fig. 2 shows the micrographs of Al-mordenite, Fe25%-substituted mordenite, Fe50%-substituted mordenite, Fe75%-substituted mordenite, and Fe-mordenite. It was observed that the crystal size of Fe-substituted Al-mordenite decreased with the increase of Fe-content in Al-mordenite. Al-mordenite crystal was tablet-like with approximately 20–30  $\mu\text{m}$  in diameter and 5–10  $\mu\text{m}$  in thickness. Fe-mordenite was fiber-like and grew up to 30  $\mu\text{m}$  in length and 5  $\mu\text{m}$  in diameter. However the morphology of Fe-substituted Al-mordenites was cubic-like with 5–10  $\mu\text{m}$  in size and their size was smaller than Al-mordenite and Fe-mordenite. These observations suggest that the replacement of Al by Fe inhibited the crystal growth of mordenite, compared with Al-mordenite and Fe-mordenite. According to the reports on natural zeolites, the morphology of natural mordenite with small amount of impurities was needle-like or fiber-like with *c*-axis elongation [11]. Therefore, the considerable effect of the Fe substitution on the morphology of crystal leads to the indications of Fe-incorporation into the framework of Al-mordenite. Fig. 3 shows the typical results of TG-DTA for Al-mordenite, Fe-mordenite and Fe25%-substituted mordenite. TEA as a template was decomposed in air at 440–450°C for Al-mordenite and Fe-mordenite by TG-DTA, as shown in Fig. 3. On the contrary Fe-substituted Al-mordenites indicated the lower peak temperature of decomposition of TEA than that of Al-mordenite and Fe-mordenite. The reason on this distinction between peak temperature is under investigation.

The X-ray diffraction (XRD) patterns of Al-mordenite and Fe-mordenite are shown in Fig. 4. Both Al-mordenite and Fe-mordenite revealed high crystallinity, as shown in Fig.4. Fe-mordenite showed the XRD pattern similar to that of Al-mordenite. No other diffraction peaks caused by other phases were observed for Fe-mordenite. The diffraction peaks for Fe-mordenite could be indexed by the assumption of the same structure as Al-mordenite. There was no obvious difference in the crystallinity for Al-mordenite and Fe-mordenite. Also the results of XRD for Al-mordenites with various Fe-contents are shown in Fig. 4. XRD patterns for various Fe-containing Al-mordenites synthesized in this process indicated the same XRD patterns as Al-mordenite and Fe-mordenite and any peaks of diffraction due to other crystalline materials were not observed. Wu *et al.* also showed that for Fe-containing mordenites synthesized hydrothermally without an organic template Fe-substitution into the framework of Al-mordenite has occurred [8]. Also, the report about the solid solution of Be into Al-mordenite by Ueda *et al.* indicated that the diffraction peaks for Be/Al-mordenite could be indexed by the assuming the same orthorhombic cell as Al-mordenite [6], and therefore it was concluded that Al<sup>3+</sup> ion could be substituted with Be<sup>2+</sup> ion [12]. In this work it is likely that the replacement of Al with Fe in Al-mordenite maintains the framework of Al-mordenite because the X-ray data confined that the structure of mordenite was stable even when all of Al is replaced Fe in Al-mordenite.

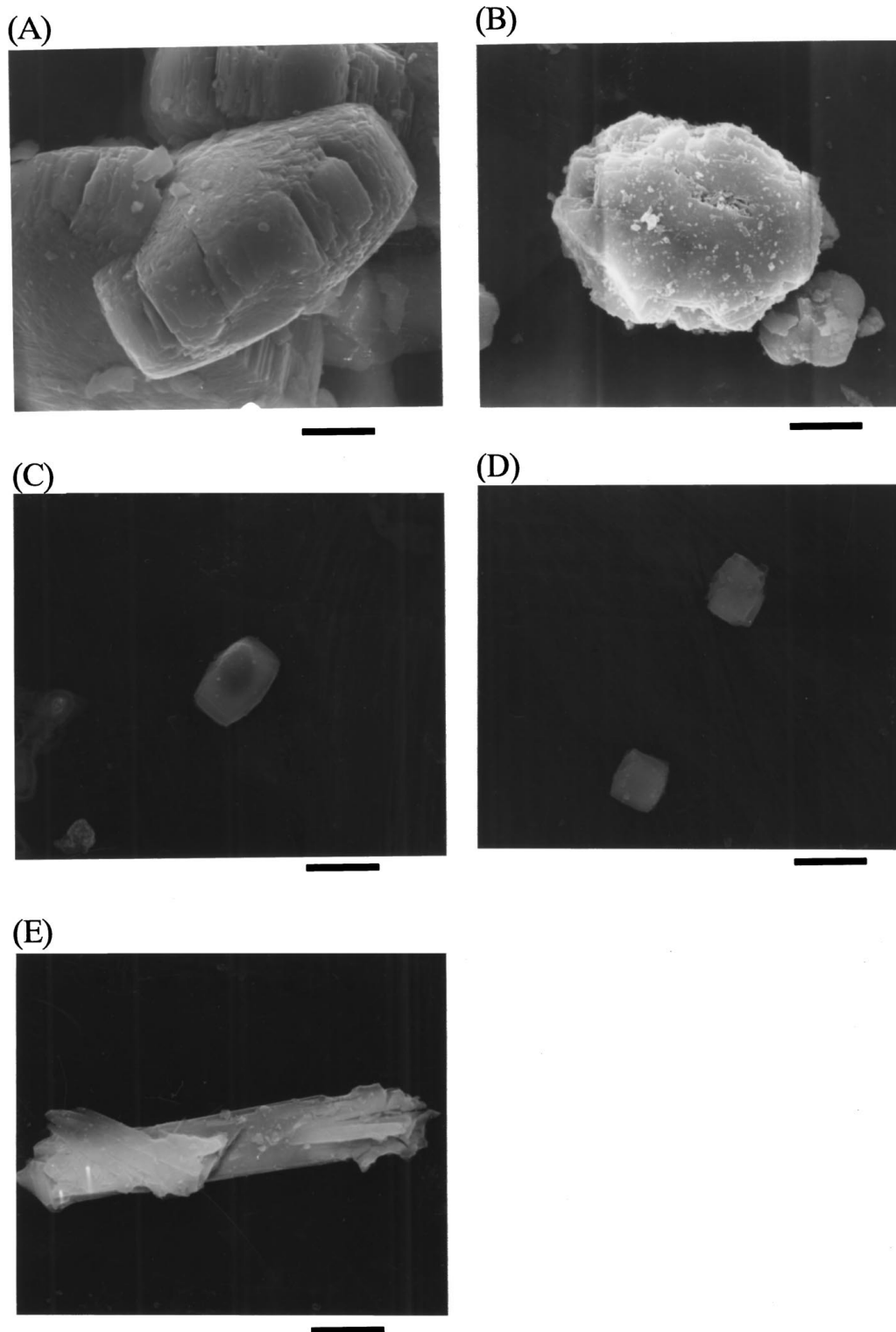


Figure 2 SEM photographs of Al-mordenite (A), Fe25%-substituted mordenite (B), Fe50%-substituted mordenite (C), Fe75%-substituted mordenite (D), and Fe-mordenite (E). Bars show 5  $\mu\text{m}$ .

Fig. 5 shows the lattice constants,  $a$ ,  $b$  and  $c$ , of Al-mordenite, Fe-mordenite and Fe-substituted Al-mordenites. Fe-mordenite possessed the almost same values of  $a$ ,  $b$ , and  $c$  as Al-mordenite. On the other hand, Fe-substituted Al-mordenites showed the smaller values of  $a$ ,  $b$ , and  $c$  parameters than Al-mordenite. However, Wu reported that the values of unit cell parameters increased gradually with increasing Al replacement for Fe-substituted mordenites, which could lead to the presence of tetrahedral  $\text{Fe}^{3+}$  in Fe-substituted Al-mordenite with free template [8]. Because  $\text{Fe}^{3+}$

has a larger ionic radius than  $\text{Al}^{3+}$ , the lattice constants,  $a$ ,  $b$ , and  $c$ , must be increased with the substitution of  $\text{Fe}^{3+}$  (ion radius: 0.063 nm) for  $\text{Al}^{3+}$  (ion radius: 0.053 nm) in Fe-substituted mordenites, as shown by Wu *et al.* However, these results of lattice parameters in the present experiment were in conflict with the tendency reported by Wu [8]. Lattice parameters of mordenites decreased with increasing silica content, i.e., higher Si/Al ratio, which was reported by Ueda *et al.* [13,6]. Fig. 6 shows the ratio of  $\text{SiO}_2/(\text{Al}_2\text{O}_3 + \text{Fe}_2\text{O}_3)$  with incorporation of Fe into

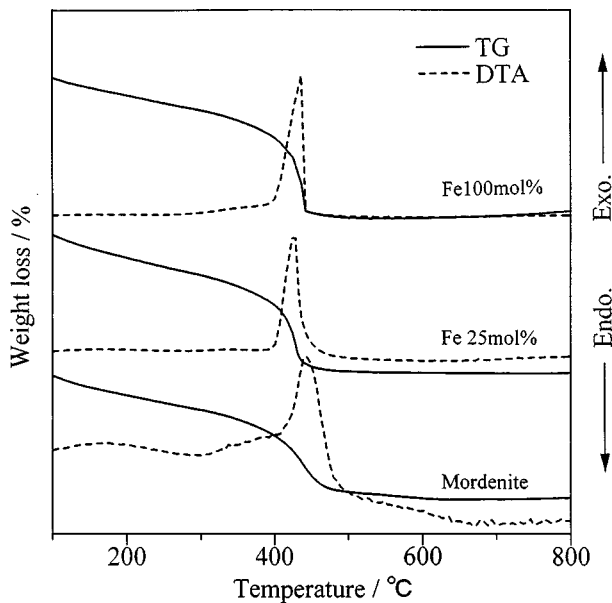


Figure 3 Typical results of TG-DTA for Al-mordenite, Fe-mordenite and Fe25%-substituted mordenite.

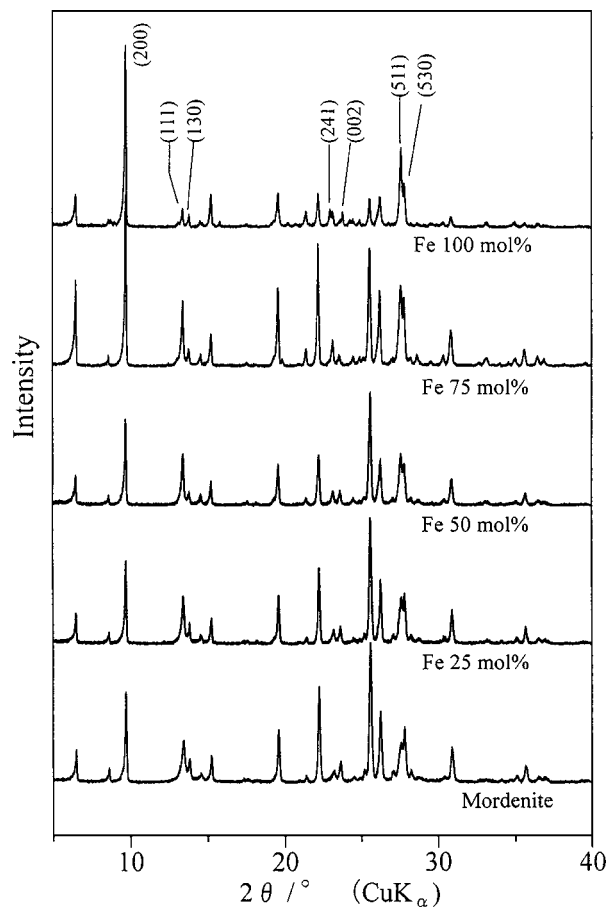


Figure 4 X-ray diffraction (XRD) patterns of Al-mordenite, Fe-mordenite and Fe-substituted Al-mordenites.

Al for Al-mordenites. Ratio of  $\text{SiO}_2/(\text{Al}_2\text{O}_3 + \text{Fe}_2\text{O}_3)$  was found to be around 13 and quite constant with Fe content for Fe-substituted Al-mordenites. Ideally the ratio of  $\text{SiO}_2/\text{Al}_2\text{O}_3$  for Al-mordenite was 10. Therefore, the decrease in the lattice parameters,  $a$ ,  $b$ , and  $c$  of Fe-substituted Al-mordenites may be explained by this high silica ratio.

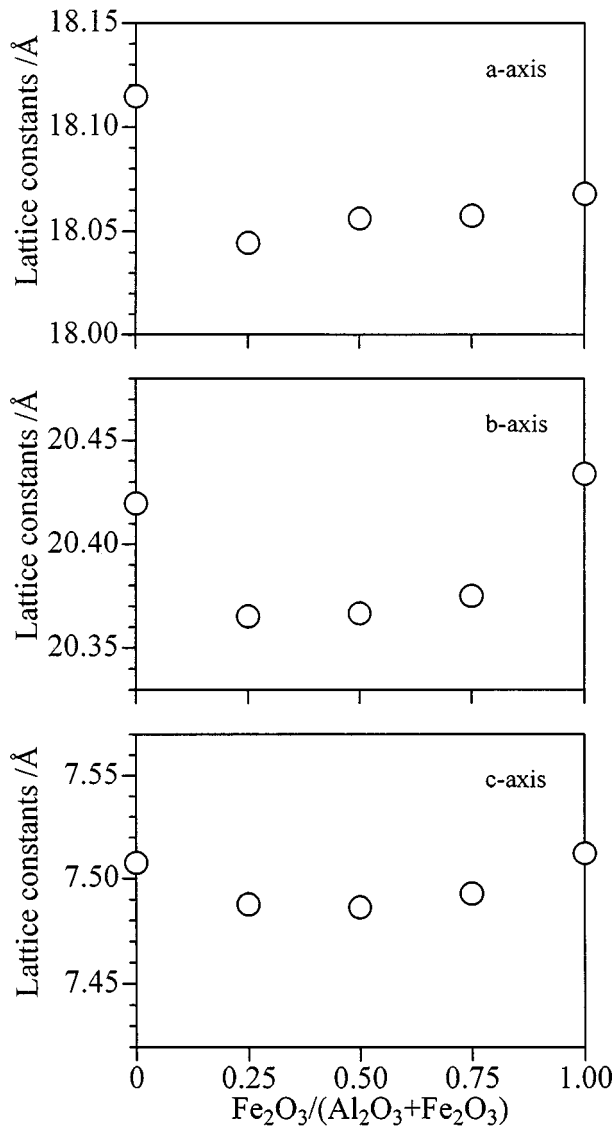


Figure 5 The lattice parameter of Al-mordenite, Fe-mordenite and Fe-substituted Al-mordenites.

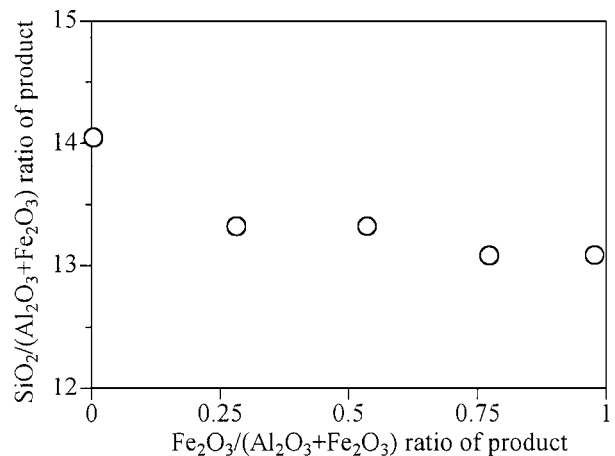


Figure 6 Variation of ratio of  $\text{SiO}_2/(\text{Al}_2\text{O}_3 + \text{Fe}_2\text{O}_3)$  with incorporation of Fe into mordenites.

The results of Raman spectra for Al-mordenite with various substitution of Fe for Al are shown in Fig. 7. A peak at  $820\text{ cm}^{-1}$  was identified for Al-mordenite, although Fe-substituted Al-mordenites and Fe-mordenite indicated the broad peak at  $800\text{--}820\text{ cm}^{-1}$  region. This broad peak of Fe-substituted Al-mordenites and

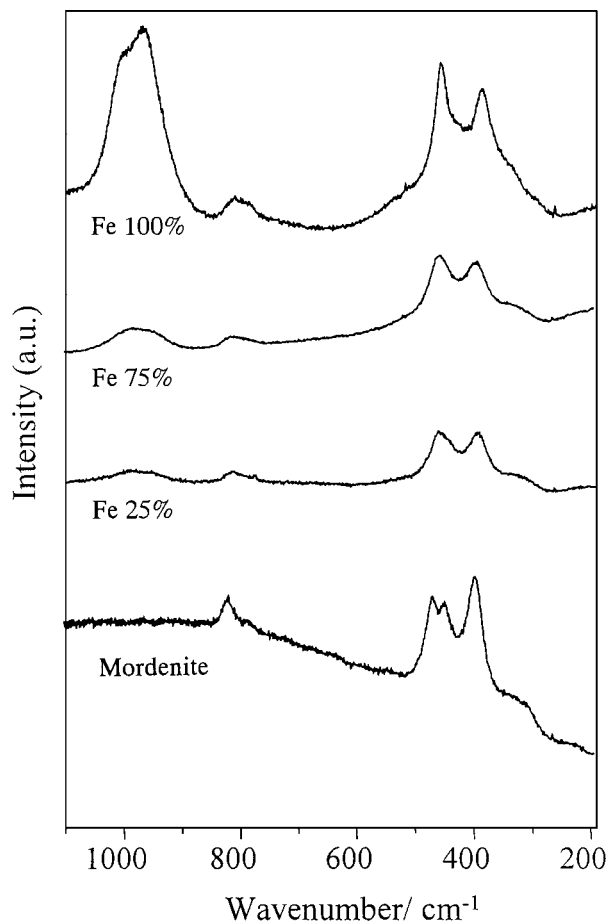


Figure 7 Raman spectra for Al-mordenite, Fe-mordenite and Fe-substituted Al-mordenites.

Fe-mordenite at 800–820  $\text{cm}^{-1}$  region was attributed to a stretching vibration mode of  $\text{SiO}_4$  [14]. On the contrary in the spectra of Fe-mordenite and Fe-substituted Al-mordenites, a very distinguished peak around 1000  $\text{cm}^{-1}$  was observed. Scarano *et al.* reported that Raman spectra of Fe-silicalite with partially Fe substitution in the framework had a prominent peak at 1020  $\text{cm}^{-1}$ , which band must be considered as the fingerprint of Fe-silicalite [15]. They suggested that this peak at 1020  $\text{cm}^{-1}$  band could be associated with  $\text{FeO}_4$  stretching in the framework of silicalite. Consequently the distinguished peak around 1000  $\text{cm}^{-1}$  observed for Fe-substituted Al-mordenites and Fe-mordenite was ascribed to  $\text{FeO}_4$  stretching mode in the mordenite framework. These Raman results can be taken as significant evidence for substituting Fe for Al into the mordenite structure for Fe-mordenite and Fe-substituted mordenites.

#### 4. Summary

Al-mordenite, Fe-mordenite and Fe-substituted Al-mordenites in the  $\text{Na}_2\text{O}-\text{Al}_2\text{O}_3-\text{Fe}_2\text{O}_3-\text{SiO}_2-\text{H}_2\text{O}$  system with the tetraethylammonium as a template were synthesized hydrothermally. The replacement of Al in Al-mordenite by Fe was systematically attempted. X-ray fluorescence results were in conformity with ideal values of  $\text{Fe}_2\text{O}_3$  content. From TG-DTA result, TEA as a template was completely decomposed in air at 440–450°C for Al-mordenite and

Fe-mordenite. Fe-substituted Al-mordenites showed the lower peak temperature of decomposition of TEA than that of Al-mordenite and Fe-mordenite.

Al-mordenite crystal was tablet-like with 20–30  $\mu\text{m}$  in diameter and 5–10  $\mu\text{m}$  in thickness. Fe-mordenite was fiber-like and grew up to 20–30  $\mu\text{m}$  in length and 5  $\mu\text{m}$  in diameter. Fe-substituted Al-mordenite was cubic-like with 5–10  $\mu\text{m}$  in size. The size of Fe-substituted Al-mordenite decreased with increasing Fe-content in Al-mordenite.

Fe-substituted Al-mordenite and Fe-mordenite showed the good crystallinity and the XRD pattern similar to that of Al-mordenite. Fe-mordenite possessed the almost same values of  $a$ ,  $b$ , and  $c$  as Al-mordenite, though Fe-substituted Al-mordenites showed the smaller values of  $a$ ,  $b$ , and  $c$  parameters than Al-mordenite.

Fe-mordenite and Fe-substituted mordenites possessed a very distinguished peak around 1000  $\text{cm}^{-1}$  in Raman spectra. This distinct peak around 1000  $\text{cm}^{-1}$  was attributed to  $\text{FeO}_4$  stretching vibration in the mordenite framework. This result indicates the possibility of substitution of Fe for Al in Al-mordenite framework. Therefore the continuous solid solution of Fe into Al-site in Al-mordenite was successfully obtained in mordenites with various Al-Fe molar ratios.

#### Acknowledgement

We would like to thank Prof. T. Tanaka at Kyoto University for the suggestion and his help in performing Raman spectra measurement.

#### References

1. D. MCCONNELL, *Am. Miner.* **37** (1952) 609.
2. V. I. SOBOLEV, G. I. PANOVA, A. S. KHARITONOV, V. N. ROMANNIKOV, A. M. VOLODIN and K. G. INOUE, *J. Catal.* **158** (1996) 486.
3. T. CHAPUS, A. TUEL, Y. BEN TAARIT and C. NACCACHE, *Zeolites* **14** (1994) 349.
4. P. S. RAGHAVAN, S. KANNAN and A. A. BELHEKAR, *Indian J. Chem.* **36A** (1997) 905.
5. J. KORATOWSKI, M. SYCHEV, V. GONCHARUK and W. H. BAUR, *Stud. Surf. Sci. Catal.* **65** (1991) 581.
6. S. UEDA, H. YAMADA, M. KOIZUMI and W. M. MEIER, *Clay Sci.* **7** (1987) 49.
7. R. SZOSTAK, V. NAIR and T. L. THOMAS, *J. Chem. Soc. Faraday Trans.* **183** (1987) 487.
8. C. T.-W. CHU and C. D. CHANG, *J. Phys. Chem.* **89** (1985) 1569.
9. A. S. KHARITONOV, G. A. SHEVELEVA, G. I. PANOVA, V. I. SOBOLEV, Y. A. PAUSKIHTIS and V. N. ROMANNIKOV, *Appl. Catal.* **98** (1993) 33.
10. P. WU, T. KOMATSU and T. YASHIMA, *Microporous and Mesoporous Mater.* **20** (1998) 139.
11. G. GOTTARDI and E. GALLI, "Natural Zeolites" (Springer-Verlag, 1965) p. 178.
12. W. M. MEIER, *Zeit. Krist.* **155** (1961) 439.
13. S. UEDA, T. FUKUSHIMA and M. KOIZUMI, *J. Clay Sci. Soc. Japan* **22** (1982) 18.
14. S. BORDIGA, R. BUZZONI, F. GEOBALDO, C. L. LAMBERTI, E. GIAMELLO, A. ZECCINA, G. LEOFANTI, G. PETRINI, G. TOZZOLA and G. VLAUCL, *J. Catal.* **158** (1996) 486.
15. D. SCARANO, A. ZEOCCHINA, S. BORDIGA, F. GEOBALDO, G. SPOTO, G. PETRINI, G. LEOFANTI, M. PADOVAN and G. TOZZOLA, *J. Chem. Soc. Faraday Trans.* **89** (1993) 4123.

Received 5 April

and accepted 18 September 2000